Generation of Quasimonoenergetic Electron Bunches with 80-fs Laser Pulses

B. Hidding,[1] K.-U. Amthor,[2] B. Liesfeld,[2] H. Schwoerer,[2] S. Karsch,[3] M. Geissler,[3] L. Veisz,[3] K. Schmid,[3,4]
J. G. Gallacher,[5] S. P. Jamison,[6] D. Jaroszynski,[5] G. Pretzler,[1] and R. Sauerbrey[2]

[1]*Institut für Laser- und Plasmaphysik, Heinrich-Heine-Universität Düsseldorf, 40225 Düsseldorf, Germany*
[2]*Institut für Optik und Quantenelektronik, Friedrich-Schiller-Universität Jena, 07743 Jena, Germany*
[3]*Max-Planck-Institut für Quantenoptik, 85748 Garching, Germany*
[4]*Department für Physik, Ludwig-Maximilians-Universität München, 85748 Garching, Germany*
[5]*Department of Physics, University of Strathclyde, Glasgow G4 0NG, United Kingdom*
[6]*School of Computing and Advanced Technologies, University of Abertay Dundee, Dundee DD1 1HG, United Kingdom*
(Received 28 November 2005; published 15 March 2006)

Highly collimated, quasimonoenergetic multi-MeV electron bunches were generated by the interaction of tightly focused, 80-fs laser pulses in a high-pressure gas jet. These monoenergetic bunches are characteristic of wakefield acceleration in the highly nonlinear wave breaking regime, which was previously thought to be accessible only by much shorter laser pulses in thinner plasmas. In our experiment, the initially long laser pulse was modified in underdense plasma to match the necessary conditions. This picture is confirmed by semianalytical scaling laws and 3D particle-in-cell simulations. Our results show that laser-plasma interaction can drive itself towards this type of laser wakefield acceleration even if the initial laser and plasma parameters are outside the required regime.

In recent years, laser-plasma accelerators have gained more ground on becoming a promising alternative to conventional large scale particle acceleration facilities based on rf technology [1–4]. In laser generated wakefields, the electrons can experience accelerating fields of several hundred GV/m [5]. This exceeds the fields of conventional accelerators by several orders of magnitude. Thus, laser-plasma accelerators can generate high-energy particles over distances of only a few hundred micrometers. Electron energies of more than 300 MeV have been achieved in experiments [6]. Generally, the generated electron beams exhibit a broad exponential spectrum and large divergence. Recent experiments have, however, demonstrated the capability of laser-plasma accelerators to produce quasi-monoenergetic and well-collimated electron bunches [7–13]. This constitutes a major advance towards the application of laser-plasma accelerators to high-energy physics, biology, or medicine.

One important mechanism responsible for the generation of monoenergetic electron bunches is the laser wakefield acceleration in the highly nonlinear broken wave regime [14]. In this case, the ponderomotive force of the laser creates a bubblelike electron void which comprises a fully broken plasma wave, supporting a strong longitudinal electric field. The laser pulse travels at the front of this structure and expels electrons, which stream around the arising cavity and can be trapped inside at a fixed phase of the longitudinal field, leading to the acceleration of electron bunches with a narrow energy spread. This phenomenon has been thoroughly explored theoretically [15,16].

The conditions for this process to occur put high demands on the driving laser. On the one hand, the pulse intensity must be above the relativistic limit to be strong enough to expel all electrons out of the laser's path. This can be quantified by the dimensionless amplitude $a_0 \gg 1$, with $a_0 = (I \times (\lambda [\mu m])^2/1.37 \times 10^{18} [WM/cm^2])^{1/2}$, I and λ being the laser intensity and wavelength, respectively. For $\lambda = 0.8$ μm, this corresponds to an intensity in the 10^{19} W/cm^2 range. On the other hand, both the transverse and the longitudinal dimensions of the laser pulse in the focus must be close to half the plasma wavelength in order to allow the formation and stability of the bubblelike structure. According to this, ultrashort laser pulses of the order of 20 fs are ideal. With longer pulses, the gas density would have to be lowered to achieve a longer plasma period, which would also scale up the necessary focal spot size as well as the pulse power for achieving the required intensities.

In this Letter, we report that this scheme for quasi-monoenergetic electron acceleration is also effective with strongly relaxed requirements on the laser pulse. In our case, 80-fs long laser pulses were tightly focused into a high-density gas jet and were self-modulated in a self-generated plasma wave [17–20]. This creates short high-intensity pulse fragments that induce quasimonoenergetic electron acceleration. The experimental findings are confirmed by particle-in-cell (PIC) simulations.

In the experiment presented here, the Jena Ti:Sa terawatt laser (JETI) was operated at 800 nm with a pulse duration of 80 fs and an energy of 0.6 J on target. The setup is displayed in Fig. 1. The pulses were focused by an $f/2.2$ off-axis parabolic mirror; the vacuum FWHM was 3.2 μm, yielding an intensity of 5×10^{19} W/cm^2 corresponding to $a_0 \approx 5$. The focal spot was positioned into the rising edge of a subsonic He gas jet with a nearly Gaussian profile of 650 μm FWHM, and a peak gas density of $n_{gas} = 4 \times 10^{19}$ cm^{-3}. Upon incidence on the jet, the laser pulse fully ionizes the gas, undergoes relativistic self-
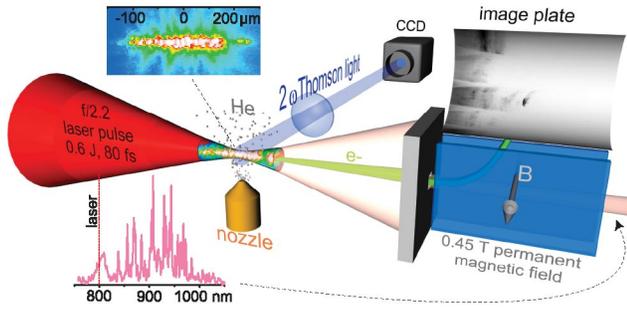
FIG. 1 (color). Experimental setup. The laser pulse is incident from the left. Nonlinear Thomson scattered light was measured perpendicular to the laser direction. Collimated electron beams were accelerated in the laser direction and analyzed by an electron spectrometer. Also in the forward direction, transmitted laser light was analyzed. The insets show an image of the nonlinear Thomson signal from the relativistic channel and a forward Raman spectrum, respectively.

focusing, and creates a plasma channel of several hundred micrometers length, which is about 10 times the Rayleigh length. Nonlinear Thomson scattering in the relativistic channel is observed perpendicular to the laser propagation direction [21]. This radiation from relativistically moving electrons in the channel is emitted near the second harmonic of the driving laser pulse [18,22,23]. It is used to measure the length and position of the plasma channel (see inset in Fig. 1).

In the laser propagation direction, an electron spectrometer equipped with permanent magnets ($B_{max} = 0.45$ T) was placed 210 mm away from the laser focus. It had a 3×5 mm^2 entrance aperture centered on the laser axis and was shielded from x rays by a combination of low- and high-Z material. Electrons were detected by an imaging plate (IP), type FUJI BAS-MS 2325. The energy calibration was done by 3D numerical tracking of electrons inside the mapped magnetic field, whereas the absolute signal intensity on the IP was determined using established dependencies including time and temperature fading [24]. Transmitted laser light could pass the electron spectrometer on axis and was analyzed by an optical spectrometer in the range of 750–1050 nm (see inset in Fig. 1).

The transverse Thomson-scattering signal and the γ dose measured by an ionization chamber placed outside the vacuum chamber were used to optimize the focus position relative to the gas jet and, hence, to the gas density profile. For most positions, exponential electron spectra were recorded. However, for a well-defined focus position the γ dose and channel length increased significantly, and electron spectra with one or two quasimonoenergetic peaks were observed, as displayed in Fig. 2. Whereas a typical exponential electron spectrum had a temperature of about 8 MeV, the peaked spectra varied strongly from shot to shot due to variations of experimental parameters. One of the spectra shows two distinct spikes at 23 and 36 MeV, while the other one exhibits a single spike at 47 MeV with 4 MeV
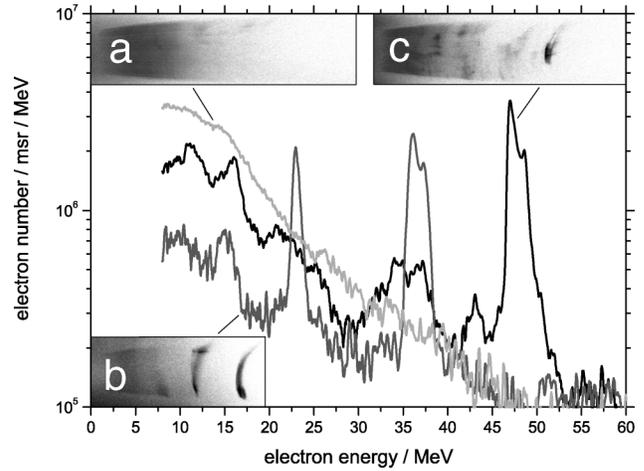

FIG. 2. Single-shot measurements: Raw data as recorded on the bent IP (insets) and extracted electron spectra. (a) Exponential spectrum with $T_{eff} = 8$ MeV; (b) double peak at 23 and 36 MeV; (c) monoenergetic peak at 47 MeV.

FWHM. This peak contains about 2×10^6 electrons and has a divergence of <10 mrad. Note that the apparent spectral width of 4 MeV is an upper limit, since broadening is also caused by the divergence of the electron beam.

When the electron spectrometer was removed, the transverse bunch profiles were recorded by a CCD camera monitoring a scintillation screen (Konica KR) 120 mm behind the focus. Without optimization, we observed a broad angular distribution. At focus positions where a strong gamma dose was recorded, the behavior changed and narrow pencil beams with a divergence angle of <10 mrad were observed (see Fig. 3). Assuming a diameter of the electron emission region of <10 μm as found by our PIC simulations, this results in a normalized transverse emittance of <8 mm mrad.
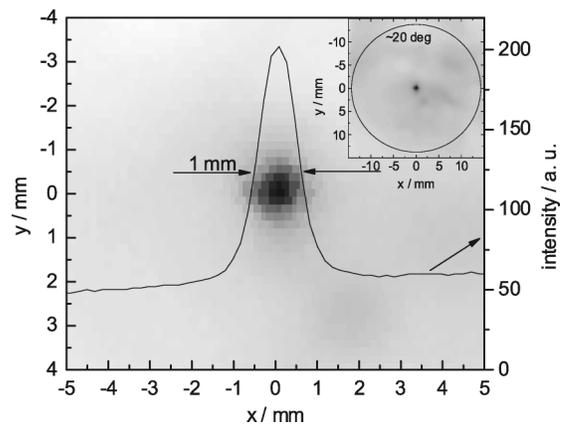

FIG. 3. Zoom of a typical image of the scintillating screen at optimum conditions. A narrow electron beam is visible. The width of 1 mm at 120 mm distance between focus and screen corresponds to an opening angle of <10 mrad. The well-collimated beam sits on top of a pedestal of electrons with a broad divergence of approximately 20° (inset).
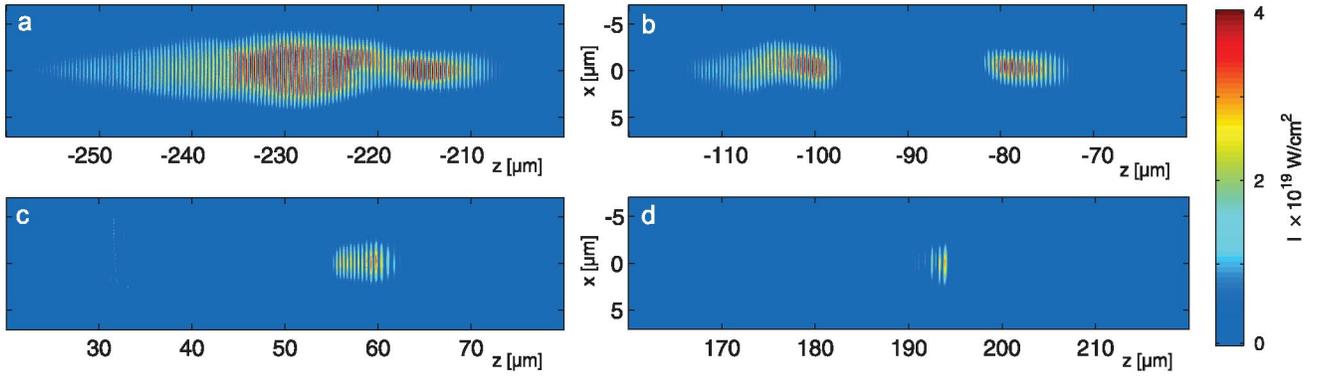
FIG. 4 (color). PIC results of the laser intensity (nonaveraged energy flux) during interaction with the underdense plasma. The snapshots are separated by 45 fs, with the Gaussian density profile of the gas jet centered around $z = 0$. The laser pulse is incident from the left and creates a relativistic plasma channel (a), is relativistically self-modulated (b), and only the first fragment survives (c) and is strong enough to accelerate quasimonoenergetic electrons (d).

For the theoretical treatment of this experimental situation, a similarity theory has recently been introduced [25] which indicates that the bubble acceleration scenario and its quasimonoenergetic electron spectra require a minimum critical laser pulse power of

$$P > P_{crit} = P_{rel}(\omega_0\tau)^2 \approx \left(\frac{\tau\,[\text{fs}]}{\lambda\,[\mu\text{m}]}\right)^2 \times 30\text{ GW}, \quad (1)$$

where $P_{rel} = m_e^2 c^5/e^2 \approx 8.5$ GW is the natural relativistic power unit, and τ and λ are the laser pulse duration and wavelength, respectively. For our laser parameters, the critical power calculates to $P_{crit} \approx 300$ TW, while the total laser power amounts to $P \approx 8$ TW. Therefore, bubble acceleration should not occur.

Thus, to analyze the underlying acceleration mechanism, 3D-PIC simulations with the ILLUMINATION code [26] were performed. The simulation box size was $144 \times 144 \times 3080$ cells with one particle per cell, corresponding to a simulated volume of $27 \times 27 \times 144\ \mu\text{m}^3$ and 64×10^6 particles. A comoving window was applied to simulate only the laser-plasma interaction region. The plasma was assumed to be fully ionized with immobile ions as a neutralizing background. The laser pulse parameters and the Gaussian density profile of the gas jet were chosen similar to the experimental data given above.

It is well known that, triggered by the stimulated forward Raman scattering (FRS) instability, a laser pulse may experience self-modulation and longitudinal energy bunching during its propagation through a gas jet [17,18,27–31]. The instability is promoted by both a high plasma density and high a_0 [29], which has been taken advantage of in our experiment by using a dense gas jet as well as strong focusing.

Indeed, the simulation reveals that the initial 80-fs laser pulse [Fig. 4(a)] is effectively modulated longitudinally by the self-excited plasma wave. At a plasma wavelength of $\lambda_p \approx 7\ \mu\text{m}$, the laser pulse breaks up [Fig. 4(b)], and, finally, after intermediate steps, only the part of the pulse

within the first plasma period survives the process and forms a 6-fs pulse fragment with about 5% of the initial pulse energy approximately 200 μm after the peak of the plasma density [Fig. 4(d)].

An experimental indication for this effect to happen was seen in the light spectra measured on axis which showed an intense and strongly modulated feature centered around 930 nm with a width of about 150 nm (see inset in Fig. 1). This signal is a signature for the self-modulation by the FRS instability and is spectrally broadened by the fragmentation and shortening of the laser pulse as well as by the spatially varying electron density.

Although only a fraction of the initial energy is contained in the remaining fragment, the pulse is now short and intense enough to fulfill the inequality (1) and to form a bubblelike accelerating structure. In Fig. 5, the electron density distribution and spectrum corresponding to the situation in Fig. 4 show the clear signature of this acceleration regime. The electrons inside the bubble constitute the peak in the spectrum. Because of the Gaussian plasma profile, the bubble is less stable than in a constant density
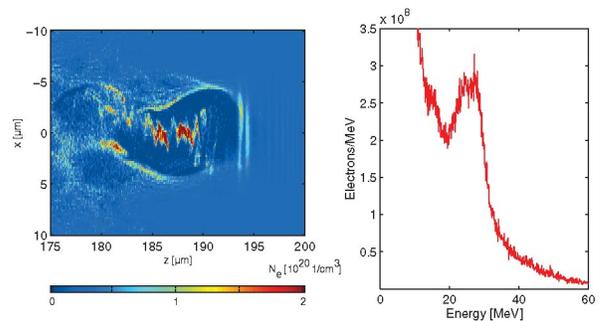

FIG. 5 (color). Electron density and spectrum for the last snapshot in Fig. 4. The diameter of the bubble is about 8 μm, and the remaining laser pulse comprises only a few cycles and is located at the front (right side) of the bubble. The electrons inside the bubble are forming the peak in the spectrum. The spectrum includes all electrons inside the simulation box.

environment, which is why after propagating another ~ 100 μm it collapses in the simulation.

The interaction of the laser pulse with a Gaussian density profile has been simulated varying the peak density. This revealed that in our case the bubble formation works for profiles with peak densities between $n_{e,\min} = 2 \times 10^{19}$ cm^{-3} and $n_{e,\max} = 1 \times 10^{20}$ cm^{-3}. This range corresponds to $\lambda_{p,\max} = 7.5$ μm and $\lambda_{p,\min} = 3.4$ μm. The reason for this is that the transverse bubble radius, for a Gaussian shaped pulse with beam waist w_0, given by $R_0 = w_0\sqrt{\ln(a_0\lambda_p(z)/w_0\pi)}$ [15] must be of the order of $\lambda_p(z)/2$, in order to form a stable bubble structure. For the given laser parameters, this condition is fulfilled in a density range of 1×10^{19} cm$^{-3} < n_e(z) < 8 \times 10^{19}$ cm^{-3}. If $n_e > n_{e,\max}$, the laser pulse reaches the necessary density range for bubble formation too early and the pulse is still too long, while, for $n_e < n_{e,\min}$, self-modulation is too slow, and, when the pulse is finally short enough, the density is too low.

The supposed acceleration process with observed maximum energies of the monoenergetic electron peaks of 10–50 MeV is confirmed by the similarity theory [25], given by $E_{\mathrm{mono}} \approx \sqrt{P_{\mathrm{mod}}/P_{\mathrm{rel}}} \times \tau_{\mathrm{mod}}$ [fs]$/\lambda$ [μm] $\times 0.1$ MeV. For example, modulated pulse fragments with an energy of ≈ 40 mJ and duration $\tau_{\mathrm{mod}} \approx 8$ fs lead to an electron energy of ≈ 24 MeV, at the same time fulfilling inequality (1) via 5 TW $>$ 3 TW. This is in good agreement with the pulse fragments observed in the simulations, where the electron peak was found to be very sensitive to changes of n_e and varies between 10–40 MeV. Additionally, the simulations showed that best acceleration results are achieved when the bubble is formed close to the density maximum, where the gradients are small enough to allow for constant conditions along the acceleration path.

Hence, experiment, theory, and simulations lead to the physical picture that the "long" laser pulse is modulated in the dense plasma, and fragments are generated which are short and strong enough to form a nonlinear bubblelike plasma region which accelerates electrons to the same energy. From PIC simulations, electron bunch durations of <10 fs are obtained.

Sometimes, double peaks appeared in the spectrum [Fig. 2(b)], which we believe to be a signature that two of the generated laser fragments are strong enough to create the effect.

We generated quasimonoenergetic electron bunches by promoting self-modulation of a 80-fs laser pulse making use of a high-density gas jet and strong focusing. The self-modulated pulse fragments are able to generate a nonlinear plasma wave in a regime where the creation of a quasimonoenergetic electron distribution takes place. Estimates on the fragments' duration and power in conjunction with

recently deduced scaling laws in the "bubble" acceleration picture describe the process semiquantitatively.

This means that, in contrast to earlier expectations, ultrashort laser pulses (<50 fs) are not necessarily required, because the plasma itself can shape the pulses to the parameters necessary for this type of quasimonoenergetic electron acceleration. This is an encouraging result for the field of laser acceleration. It shows that high-quality electron beams can be generated in a wider laser and density parameter range than indicated by previous studies, which will nurture further developments and improvements of high-quality particle beams from laser accelerators.

[1] E. Esarey *et al.*, IEEE Trans. Plasma Sci. **24**, 252 (1996).
[2] P. L. Shkolnikov *et al.*, Appl. Phys. Lett. **71**, 3471 (1997).
[3] P. Mora, Plasma Phys. Controlled Fusion **43**, A31 (2001).
[4] D. Umstadter, Phys. Plasmas **8**, 1774 (2001).
[5] V. Malka *et al.*, Science **298**, 1596 (2002).
[6] S. P. D. Mangles *et al.*, Phys. Rev. Lett. **94**, 245001 (2005).
[7] S. P. D. Mangles, Nature (London) **431**, 535 (2004).
[8] J. Faure, Nature (London) **431**, 541 (2004).
[9] C. G. R. Geddes, Nature (London) **431**, 538 (2004).
[10] V. Malka *et al.*, Phys. Plasmas **12**, 056702 (2005).
[11] K. Krushelnick *et al.*, Phys. Plasmas **12**, 056711 (2005).
[12] E. Miura *et al.*, Appl. Phys. Lett. **86**, 251501 (2005).
[13] A. Yamazaki *et al.*, Phys. Plasmas **12**, 093101 (2005).
[14] A. Pukhov and J. Meyer-ter Vehn, Appl. Phys. B **74**, 355 (2002).
[15] I. Kostyukov *et al.*, Phys. Plasmas **11**, 5256 (2004).
[16] A. Pukhov *et al.*, Plasma Phys. Controlled Fusion **46**, B179 (2004).
[17] P. Sprangle *et al.*, Phys. Rev. Lett. **69**, 2200 (1992).
[18] D. Umstadter *et al.*, Science **273**, 472 (1996).
[19] E. Esarey *et al.*, IEEE J. Quantum Electron. **33**, 1879 (1997).
[20] Z. Najmudin *et al.*, Phys. Plasmas **10**, 2071 (2003).
[21] B. Liesfeld *et al.*, Appl. Phys. B **79**, 1047 (2004).
[22] E. S. Sarachik and G. T. Schappert, Phys. Rev. D **1**, 2738 (1970).
[23] Y. Y. Lau *et al.*, Phys. Plasmas **10**, 2155 (2003).
[24] K. A. Tanaka *et al.*, Rev. Sci. Instrum. **76**, 013507 (2005).
[25] S. Gordienko and A. Pukhov, Phys. Plasmas **12**, 043109 (2005).
[26] M. Geissler, Ph. D. thesis, TU Wien, 2000.
[27] N. E. Andreev *et al.*, JETP Lett. **55**, 571 (1992).
[28] T. M. Antonsen and P. Mora, Phys. Rev. Lett. **69**, 2204 (1992).
[29] C. D. Decker *et al.*, Phys. Rev. E **50**, R3338 (1994).
[30] W. B. Mori *et al.*, Phys. Rev. Lett. **72**, 1482 (1994).
[31] C. D. Decker *et al.*, IEEE Trans. Plasma Sci. **24**, 379 (1996).